TU Delft

Delft University of Technology

Document Version
Final published version

Citation (APA)
Bertassi, M., Damiani, N., Sharma, S., Smerilli, M., Mirra, M., Lanese, I., Parisi, E. R., O'Reilly, G., Messali, F., & Graziotti, F. (2025). Out-of-plane shake-table testing of urm gable walls considering different roof configurations. In *COMPDYN 2025 - 10th International Conference on Computational Methods in Structural Dynamics and Earthquake Engineering* (pp. 879-890). (COMPDYN Proceedings). National Technical University of Athens. https://doi.org/10.7712/120125.12455.25169

Important note
To cite this publication, please use the final published version (if applicable).
Please check the document version above.

Copyright
In case the licence states “Dutch Copyright Act (Article 25fa)”, this publication was made available Green Open Access via the TU Delft Institutional Repository pursuant to Dutch Copyright Act (Article 25fa, the Taverne amendment). This provision does not affect copyright ownership.
Unless copyright is transferred by contract or statute, it remains with the copyright holder.

Sharing and reuse
Other than for strictly personal use, it is not permitted to download, forward or distribute the text or part of it, without the consent of the author(s) and/or copyright holder(s), unless the work is under an open content license such as Creative Commons.

Takedown policy
Please contact us and provide details if you believe this document breaches copyrights.
We will remove access to the work immediately and investigate your claim.

This work is downloaded from Delft University of Technology.

Available online at www.eccomasproceedia.org
Eccomas Proceedia COMPDYN (2025) 879-890

ECCOMAS
Proceedia

COMPDYN 2025
10th ECCOMAS Thematic Conference on
Computational Methods in Structural Dynamics and Earthquake Engineering
M. Papadrakakis, M. Fragiadakis (eds.)
Rhodes Island, Greece, 15-18 June 2025

OUT-OF-PLANE SHAKE-TABLE TESTING OF URM GABLE WALLS CONSIDERING DIFFERENT ROOF CONFIGURATIONS

Marta Bertassi[1], Nicolo Damiani[2,3], Satyadhrik Sharma[4], Marco Smerilli[3], Michele Mirra[4], Igor Lanese[3], Elisa Rizzo Parisi[3], Gerard O'Reilly[1,3], Francesco Messali[4], Francesco Graziotti[2,3]

[1] University School for Advanced Studies IUSS Pavia
Pavia, Italy
{marta.bertassi, gerard.oreilly}@iusspavia.it

[2] Department of Civil Engineering and Architecture (DICAr), University of Pavia
Pavia, Italy
{nicolo.damiani, francesco.graziotti}@unipv.it

[3] European Centre for Training and Research in Earthquake Engineering EUCENTRE
Pavia, Italy
{marco.smerilli, igor.lanese, elisa.rizzoparisi}@eucentre.it

[4] Faculty of Civil Engineering and Geosciences, University of Technology of Delft (TU Delft)
Delft, the Netherlands
{S.Sharma-9, M.Mirra, F.Messali}@tudelft.nl

Abstract

Typical low-rise masonry buildings worldwide often feature unreinforced masonry (URM) walls paired with pitched roof configurations supported by masonry gables. Past earthquakes indicate that these components are vulnerable to out-of-plane seismic loads. This study presents key findings from the experimental campaign of the ERIES SUPREME project, which aims to advance understanding of the out-of-plane seismic response of masonry gables. Incremental dynamic tests simulating induced and tectonic seismicity scenarios were conducted on three full-scale URM gables, using two shake tables. Differential motions applied to the top and bottom tables allowed the simulation of gable interaction with distinctly different roof configurations. The experimental results are presented in terms of failure mechanisms, force-displacement hysteresis behavior, and acceleration and displacement capacities. These findings will contribute to refining and calibrating existing numerical models.

Keywords: Gable walls, Incremental dynamic shake-table tests, Out-of-plane, Roof stiffness, Unreinforced masonry, Differential input motions.

ISSN:2623-3347 © 2025 The Authors. Published by Eccomas Proceedia.
Peer-review under responsibility of the organizing committee of COMPDYN 2025.
doi: 10.7712/120125.12455.25169

1 INTRODUCTION

Unreinforced masonry (URM) structures represent a substantial portion of the global building stock, particularly in regions prone to seismic activity, including both natural earthquakes and induced seismicity. A characteristic feature of many low-rise masonry buildings is the presence of URM walls paired with various timber roof configurations, commonly supported by masonry gables. Among the structural components, masonry gables are frequently identified as highly vulnerable to out-of-plane (OOP) failure during seismic events. Post-earthquake damage assessments worldwide provide extensive evidence of this susceptibility [1]-[4], which is primarily attributed to their pronounced slenderness, weak connections to the roof structure, and their exposed position at the top of the building. This location subjects them to amplified seismic excitation compared to the motion at the ground while experiencing reduced vertical overburden loads. Additionally, the interaction between gables and flexible timber roof diaphragms can intensify vulnerability, as roof elements may amplify seismic motion rather than offer effective restraint.

Despite the well-documented seismic vulnerability of URM gables, dedicated experimental studies [5], [6] focusing specifically on their dynamic response remain scarce in the literature. Most existing research is based on tests conducted on rectangular masonry walls [7]-[13], leaving a significant gap in understanding the seismic behavior of gables. To bridge this gap, this study presents a comprehensive experimental campaign involving full-scale, densely instrumented URM gables subjected to dynamic shake-table testing until complete collapse. The tested specimens, along with their material properties, are thoroughly characterized. While the roof structure was not included in the experimental setup, its stiffness was accounted for by implementing differential input motions through an innovative dual shake-table configuration. One shake table was positioned at the gable base and another at its top, simulating realistic seismic effects.

The testing protocol incorporated input motions representative of both tectonic and induced seismicity, with an incremental dynamic loading sequence designed to capture the progressive failure mechanisms of the gables. The study ultimately presents and analyzes the experimental findings, offering new insights into the seismic behavior of URM gables and their interaction with varying roof stiffness conditions. These results contribute to a more comprehensive understanding of URM gable performance under seismic loading and provide valuable data for improving seismic assessment strategies.

The dataset of this experimental campaign, including comprehensive details on the testing setup, instrumentation schemes, and material characterization results is openly available for download from the Built Environment Data database at https://doi.org/10.60756/euc-1avy7q49 [14]. The videos of each test are also available in the same dataset, offering a visual reference for the observed structural response throughout the testing sequence.

2 GEOMETRY AND MECHANICAL CHARACTERIZATION OF THE MASONRY SPECIMENS

2.1 Specimen geometry

The test specimens of the experimental campaign consisted of three identical full-scale URM gable walls, constructed on a composite steel-concrete foundation designed for attachment to the bottom shake table of the 9D LAB of the EUCENTRE facilities in Pavia (Italy). Each wall measured 6 meters in length, and 3 meters in height, with a thickness of 105 mm (Figure 1).

The gables were built using clay bricks with dimensions of 230×105×55 mm. Each gable consisted of 45 brick courses with 10-mm-thick mortar joints. Additionally, five joist pockets

were incorporated to accommodate timber beams measuring 100×200 mm in cross-section, which were used to transfer the vertical load representative of the roof diaphragm weight. The total overburden at the mid-height of the gable was 0.07 MPa. Hence, a vertical load of 4.5 kN was applied through each timber beam, resulting in a total vertical load of 22.5 kN, simulating half the weight of a typical timber roof diaphragm, consistent with the geometry of the tested gable specimen. These beams were also used to apply lateral loads along the height of the specimen, as further discussed in the following sections.

Moreover, the experimental tests were performed without steel anchors connecting the timber joists to the masonry gables. This setup simulated a "worst-case" scenario, where the timber-to-masonry connections depended only on friction.

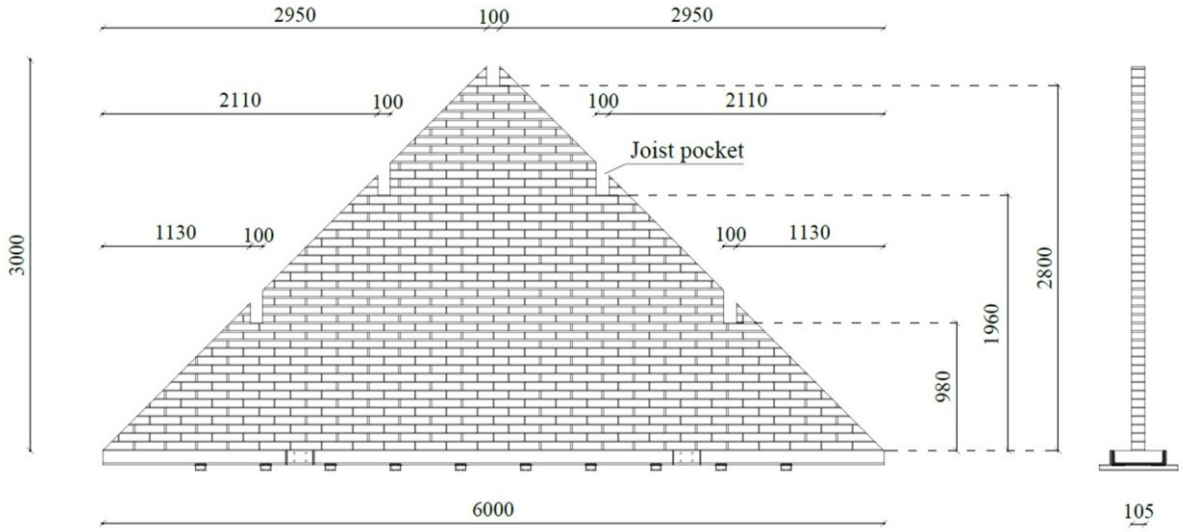


Figure 1: Full-scale masonry gable specimen details. Units of mm.

2.2 Mechanical characterization

The full-scale masonry gables tested on the 9D LAB shake table were supplemented by comprehensive material characterization of the masonry components, including individual units, mortar, and small-scale masonry specimens. This characterization involved assessing the compressive strength (f_c) and flexural strength (f_t) of the mortar, the compressive strength (f_u) of the bricks, and the compressive strength (f_m)of the masonry perpendicular to the bed joints. Additionally, the secant elastic modulus (E_m) was calculated between 10% and 33% of f_m, along with the bond strength (f_w), initial shear strength (f_{v0}), and friction coefficient (μ). All tests were conducted in accordance with the latest applicable European standards [15]-[19]. Furthermore, a specialized test [20] was performed to evaluate the response of masonry bed joints under torsional shear stress ($f_{v0,tor}$, μ_{tor}), assuming a linear elastic hypothesis. The masonry density (ρ_m) was determined based on the average weight of the three tested gables.

All the material characterization tests were carried out at the “Giorgio Macchi” Material and Structural Testing Laboratory within the Department of Civil Engineering and Architecture (DICAr) at the University of Pavia (Italy). A summary of the material properties obtained is presented in Table 1.

Material properties	Symbol	Units	Mean	C.o.V.
Mortar compressive strength	f_c	[MPa]	0.68	0.26
Mortar flexural strength	f_t	[MPa]	0.20	0.50
Unit/brick compressive strength	f_u	[MPa]	42.57	0.09
Masonry compressive strength	f_m	[MPa]	7.44	0.10
Masonry elastic modulus	E_m	[MPa]	4072	0.11
Masonry initial shear strength	f_{v0}	[MPa]	0.19	-
Masonry friction coefficient	μ	[-]	0.51	-
Masonry bond strength	f_w	[MPa]	0.21	0.48
Masonry initial shear strength (torsional)	$f_{v0,tor}$	[MPa]	0.42	-
Masonry friction coefficient (torsional)	μ_{tor}	[-]	1.15	-
Masonry density	ρ_m	[kg/m^3]	1883	-

Table 1: Summary of masonry, unit, and mortar mechanical properties.

3 TESTING SETUP, INSTRUMENTATION, AND APPLIED TESTING PROTOCOL

Three dynamic shake-table tests on full-scale masonry gables were conducted at the EUCENTRE laboratory in Pavia, Italy, using the 9D LAB facility. This advanced seismic testing system features a dual shake-table configuration, with a top and bottom table capable of applying differential input motions across nine degrees of freedom, allowing for the reproduction of interstorey displacements observed during earthquakes.

Although the 9D LAB in-plan dimensions (i.e., 4.8×4.8 m) were sufficient for testing full-scale masonry gables, they could not accommodate an entire roof diaphragm structure. To account for the influence of roof stiffness on the seismic OOP response of the gables, the input motion imposed on the top table was varied. Three different roof configurations were tested: (i) Gable1-STIFF, representing a rigid roof diaphragm, where the top table replicated the motion of the bottom table; (ii) Gable2-SEMIFLEX, representing an intermediate case, where the top motion was linearly amplified relative to the base motion; and (iii) Gable3-FLEX, simulating a flexible roof diaphragm, which resulted in significant amplification and phase shift at the gable top. This paper reports results corresponding to only Gable1-STIFF and Gable3-FLEX.

3.1 Testing setup

The experimental setup, as previously mentioned, featured a dual shake-table configuration with top and bottom tables able to apply differential input motions. The three-dimensional view of the testing setup with the components is displayed in Figure 2.

A custom-designed loading frame, constructed using tailored steel profiles, was integrated into the setup to simulate the influence of the roof structure. This loading frame imposed accelerations along the gable height through five horizontal loading arms, each hinged to the frame. To replicate real roof conditions, timber beams were attached to the steel arms, representing typical roof timber joists. Additionally, the five loading arms facilitated the application of vertical loads via springs, one per arm. To prevent any unintended out-of-plane stiffness or strength from affecting the gable specimen, the loading frame was hinged at both the top and bottom shake tables. The gable concrete foundation was securely fixed to the bottom shake table, ensuring easily numerically reproducible boundary conditions. A rigid instrumentation frame, anchored to the bottom shake table, provided support and served as a fixed reference for the measuring instruments. A key aspect of this setup was the precise control of boundary conditions, ensuring that the seismic response of each masonry gable remained independent of the loading frame.

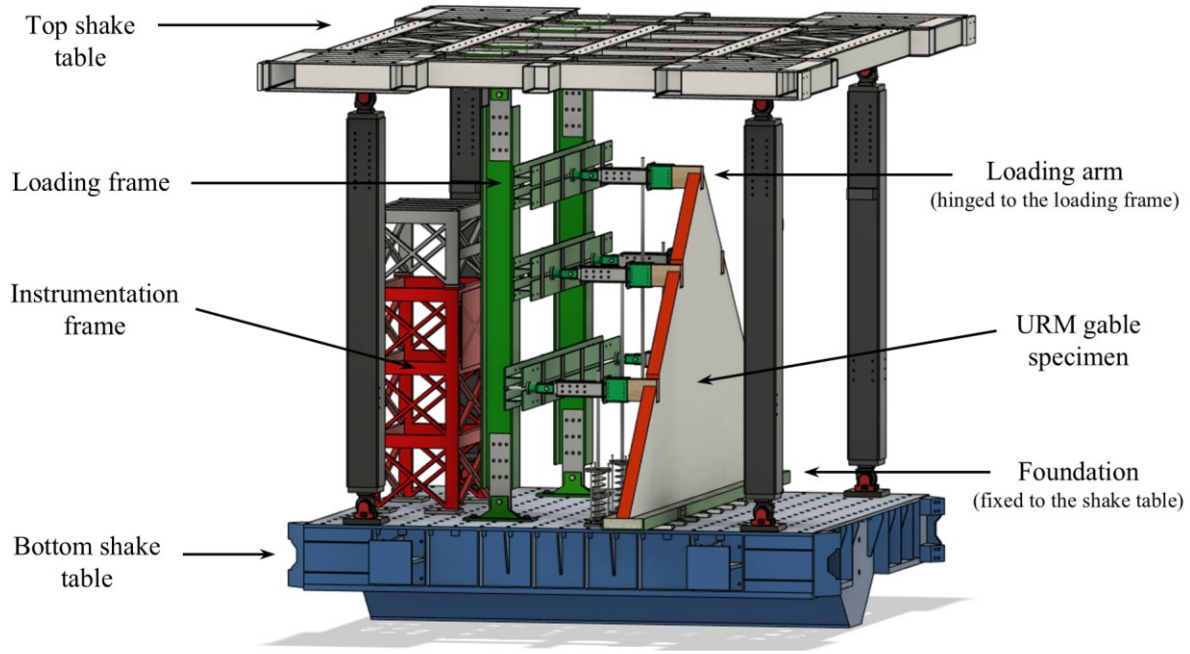


Figure 2: Three-dimensional view of the shake-table testing setup of the 9D LAB.

3.2 Instrumentation and data acquisition

The instrumentation utilized for the three gable specimens comprised accelerometers, potentiometers, wire potentiometers, and a 3D optical acquisition system. The placement of these instruments was determined based on the anticipated deformation patterns and crack propagation of the gables. Accelerometers were affixed to the gable specimens to capture acceleration-time histories, with additional units installed on the loading and instrumentation frames, as well as on the specimen foundation. Traditional potentiometers measured the elongation or contraction of springs and the relative displacements between the timber beams and the masonry. Wire potentiometers, connected to both the loading and instrumentation frames, tracked the displacements of the gable specimens. Lastly, the optical monitoring system was used to measure displacements on the free surface of the URM gable specimen, opposite the loading frame.

3.3 Input signals and testing protocols

The 9D LAB setup facilitated the application of different input motions to the bottom and top shake tables, simulating the effect of the roof diaphragm in-plane stiffness. Two distinct floor motion (FM) scenarios were considered: FM1, representing induced seismicity, and FM2, associated with tectonic seismicity. A summary of the elastic response spectra for both scenarios is presented in Figure 3. Further details regarding the selection of input signals and their variation based on different roof typologies can be found in [21].

Each gable specimen was submitted to an incremental dynamic test (IDT) using both FM1 and FM2 input signals. The testing protocol involved first applying FM1 with scaling factors (SF) of 10%, 20%, 30%, 50%, 75%, and 100%, followed by FM2, which was tested with SF of 50%, 75%, 100%, 125%, 150%, 175%, 200%, 250%, 300%, and 350%. These SF were linearly adjusted based on the bottom input signal. For Gable3-FLEX, the recorded relative displacement of the ridge beam with respect to the bottom shake-table, was equal to 5.9 mm, 12.1 mm, 16.0 mm, 26.7 mm, 39.8 mm, 52.8 mm, 40.4 mm, 57.0 mm, 85.9 mm, 107.5 mm, and 112.2 mm for each testing run, respectively (note that Gable3-FLEX collapsed at SF=150% of FM2).

To preliminary characterize the dynamic response of the specimens, several intensity measures for SF=100% were considered. The peak bottom acceleration (*PBA*), which represents the maximum acceleration applied at the base of the specimens, was 0.42 g for FM1 and 0.54 g for FM2. The peak ridge acceleration (*PRA*), indicating the maximum acceleration at the ridge level of the gables, varied depending on the floor motion scenario and gable specimen. Under FM1, Gable2-SEMIFLEX had a *PRA* of 0.75 g, while Gable3-FLEX reached 1.19 g. When subjected to FM2, these values increased to 0.96 g for Gable2-SEMIFLEX and 1.33 g for Gable3-FLEX. Additionally, the significant duration ($D_{5\text{-}95}$) for FM1, at the attic floor level was 2.92 seconds, a value that remained consistent across all specimens. At the ridge level, the same duration was observed for Gable1-STIFF and Gable2-SEMIFLEX, whereas Gable3-FLEX experienced a longer duration of 4.23 seconds. Under FM2, the significant duration at the attic floor level, as well as at the ridge level of Gable1-STIFF and Gable2-SEMIFLEX, was recorded as 7.55 seconds. In contrast, Gable3-FLEX exhibited an extended duration of 10.5 seconds at the ridge level.

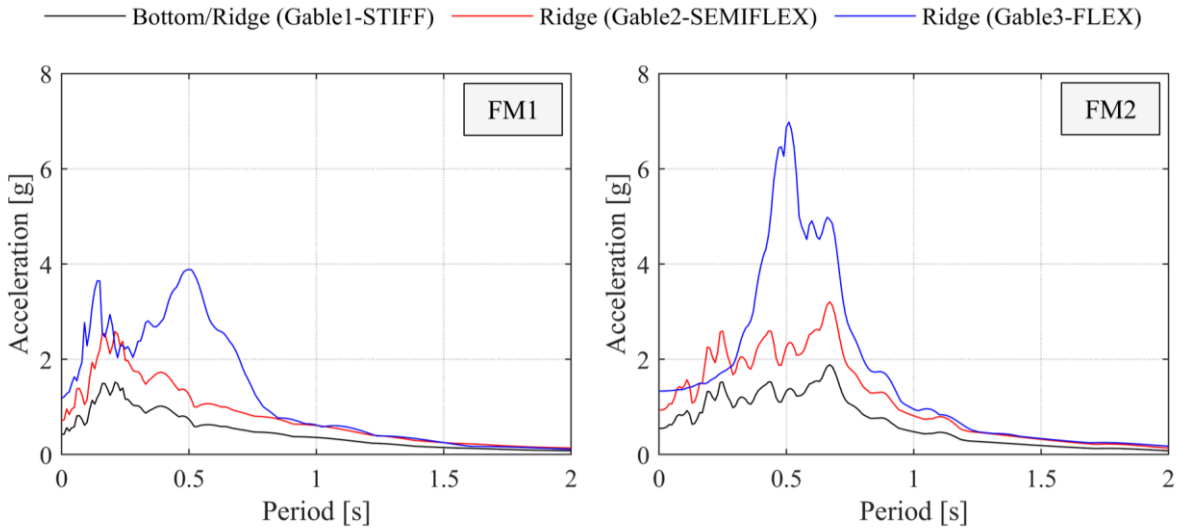


Figure 3: Summary of elastic response spectra for 5% viscous damping ratio at SF=100%.

4 RESULTS

The results of the full-scale shake-table experiments are presented and discussed in terms of the observed failure mechanisms and the corresponding incremental dynamic response. This paper focuses exclusively on the results of Gable1-STIFF and Gable3-FLEX representing the two extreme cases in terms of roof flexibility among the three tested specimens. Both specimens were tested till collapse, which happened at SF=350% of FM2 for the former, and at SF=150% of FM2 for the latter.

4.1 Crack patterns and failure mechanisms

Both tested gables exhibited a one-way bending failure mechanism, ultimately leading to complete collapse. This failure was preceded by a three-body rocking mechanism, which developed around hinges formed by two horizontal flexural cracks. These cracks extended across the entire length of the gable at the locations of the two sets of timber joists. For all the gables, minor damage was observed after the initial test at 10% FM1 scaling. This damage manifested as a horizontal crack along the gable base, although it remains uncertain whether this crack was

pre-existing. A thorough visual inspection was conducted after each test to identify and document all cracks. Figures 4 and Figures 5 illustrate the observed crack patterns, where newly formed cracks following the specified test are highlighted in blue, while cracks from previous loading cycles are represented in black.

In the case of Gable1-STIFF (Figure 4), light damage was observed only after the test at 50% FM1. This was a horizontal crack below one of the lower purlins in the left part of the gable. In subsequent tests, ranging from 100% FM2 to 200% FM2, the previously recorded crack propagated laterally from the left side to the right side of the gable, this crack had not yet fully developed along the full length of the gable to allow it to function as a plastic hinge. During the test at 250% FM2 this horizontal crack extended along the full length of the gable and consequently began functioning as a plastic hinge, allowing the top and bottom sections of the gable to move independently and rotate about it. Residual sliding displacements between the lower right purlin and the gable wall could also be observed at the end of this test. The subsequent test at 300% FM2 resulted in further damage, including the complete formation of an additional horizontal crack beneath the top two purlins; this new crack initiated a secondary mechanism, further compromising the integrity of the structure. Ultimately, the specimen collapsed during the test at 350% FM2.

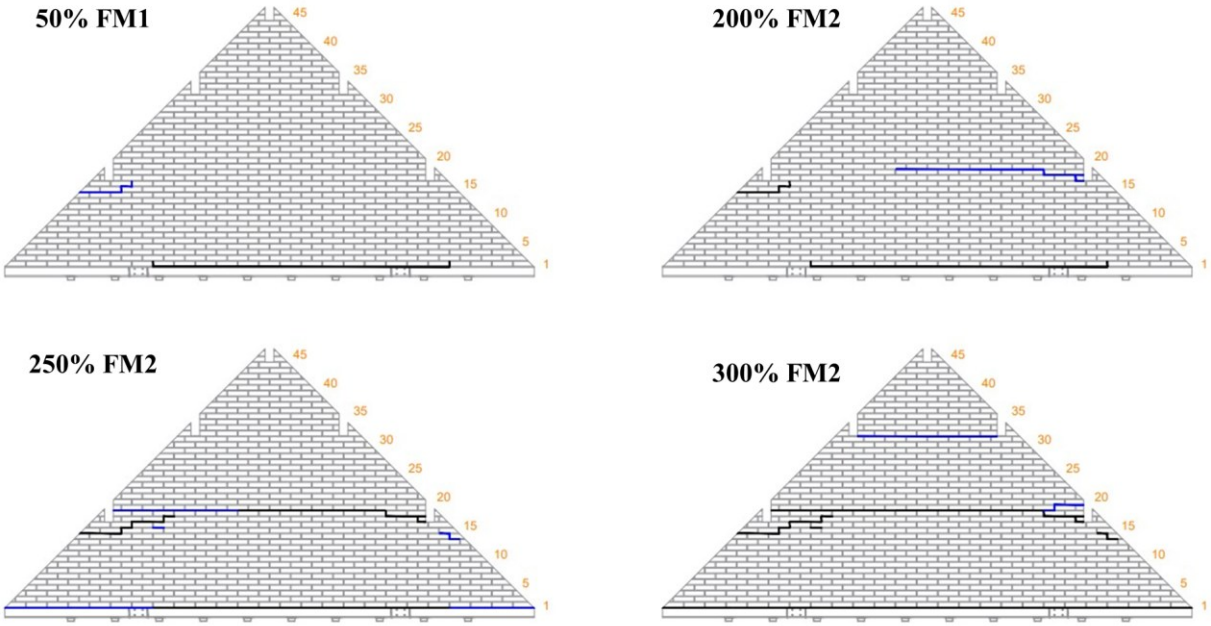


Figure 4: Progression of damage and development of failure mechanism for Gable1-STIFF.

In the case of Gable3-FLEX (Figure 5), minor cracks began to appear throughout the masonry at 50% FM1. However, these were not considered structurally significant. The horizontal crack along the gable base became fully developed when the testing intensity reached 75% FM1. At this stage, a significant crack also formed in the central part of the gable at brick level 11. As the intensity increased to 100% FM2, the gable exhibited further signs of deterioration, with new cracks emerging. A horizontal crack developed at brick level 16, running along the entire length of the gable, just above the previously identified crack. Additionally, two more horizontal cracks appeared at brick levels 30 and 33, spanning between the two purlins in the upper section of the gable. By this stage, the gable had become unstable. To evaluate the ability of the gable to withstand induced seismic motion, the testing intensity was temporarily reduced to 100% FM1(-R). This test was not performed for Gable 1-STIFF. No significant increase in

damage was observed, apart from the formation of an inclined stepped crack extending from the gable base to the horizontal crack that had formed at 75% FM1. Furthermore, no additional damage was recorded during the 100% FM2 and 125% FM2 tests. Ultimately, the gable collapsed onto the shaking table at150% FM2, a significantly lower scaling factor compared to Gable1-STIFF, which withstood testing up to 350% FM2 before failing.

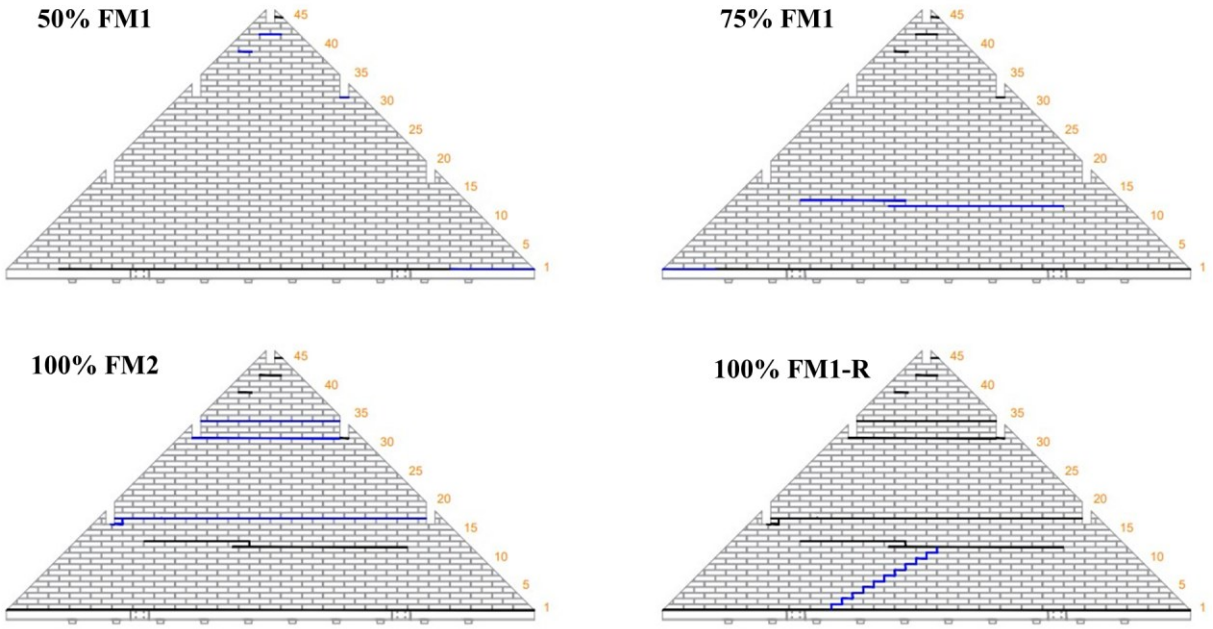


Figure 5: Progression of damage and development of failure mechanism for Gable3-SEMIFLEX.

4.2 Incremental dynamic response

The seismic capacity of the tested gables is represented through incremental dynamic testing curves, with two separate curves provided for each specimen.

The first set of curves (Figure 6a and Figure 6c) illustrates the relationship between peak bottom acceleration (*PBA*) and the corresponding maximum displacement of the control point (max(d_{ctrl})) at each acceleration level. The displacement of the control point (d_{ctrl}) represents the maximum deflection of the gable during each run, excluding any rigid-body motion from the loading frame. As damage accumulated, the location of the control point shifted, requiring trigonometric calculations to determine displacement values when direct instrumentation was not available. During the first runs of the IDT, this point was located at the gable midpoint, but as the cracks developed and the collapse mechanism was activated, its location adjusted accordingly.

The second set of curves (Figure 6b and Figure 6d) presents the average spectral acceleration ($S_{a,avg}$), computed following the methodology proposed by Kohrangi *et al.* [22]. This value is obtained by using an acceleration time history as input for the acceleration spectra, computed as the average of the bottom table and ridge beam acceleration time histories. The analysis considers a period range from 0.02 s to 0.67 s, corresponding to the elastic period of the gable at the beginning of the incremental dynamic testing sequence (~0.02 s) and the period at the end (~0.67 s).

A comparison of the capacity curves, looking at the same values of *PBA* and $S_{a,avg}$, highlights the impact of roof flexibility on the seismic response of URM gables. Gable3-FLEX

demonstrates significantly lower seismic capacity and substantially higher flexibility, indicating a marked reduction in stiffness compared to the Gable1-STIFF configuration.

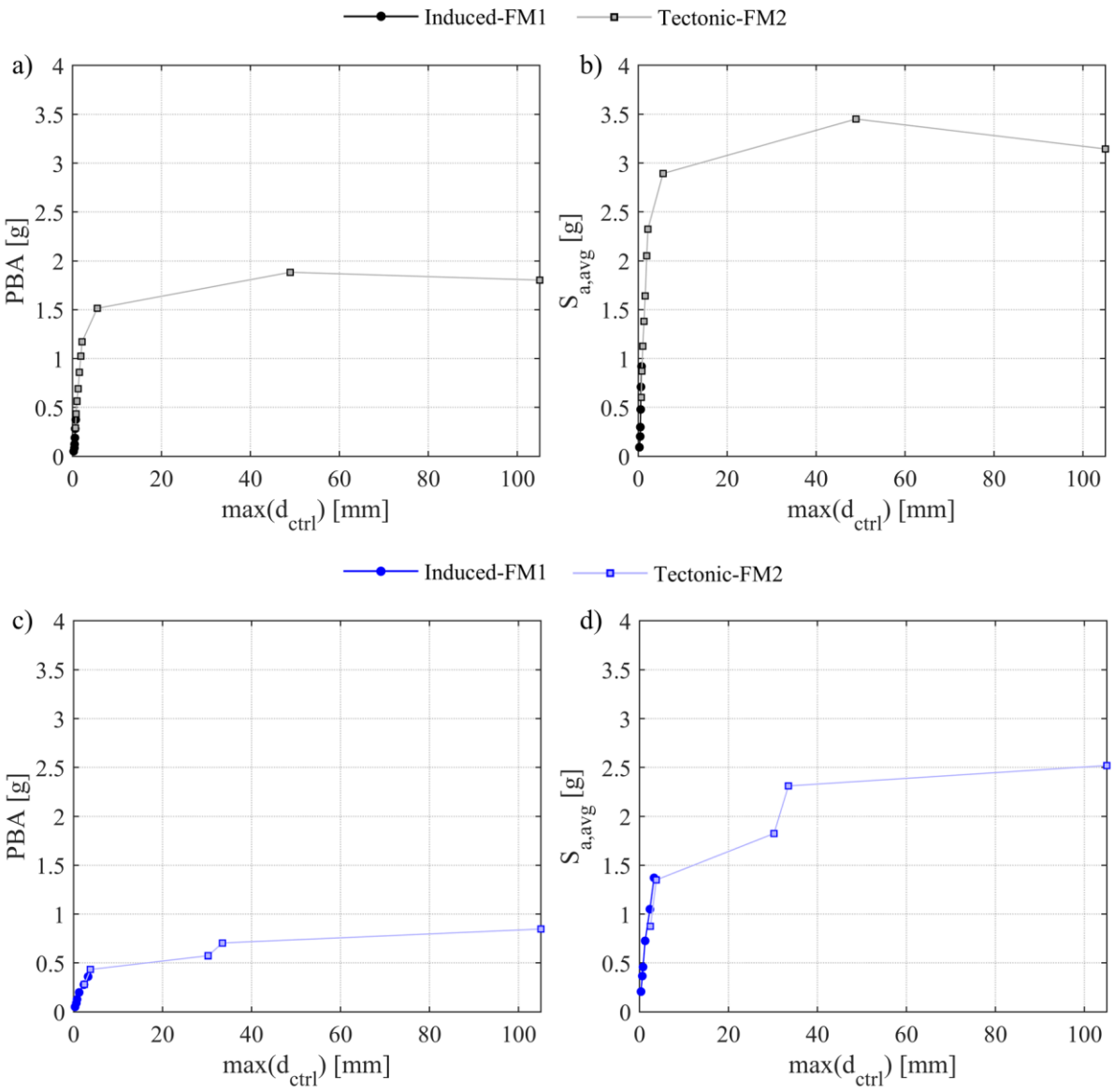


Figure 6: (a) Capacity curves of Gable1-STIFF considering PBA; (b) Capacity curves of Gable1-STIFF considering S_a,avg; (c) Capacity curves of Gable3-FLEX considering PBA; (d) Capacity curves of Gable3-FLEX considering S_a,avg.

5 CONCLUSIONS

This study presents the findings from full-scale incremental dynamic shake-table tests on unreinforced masonry (URM) gables, focusing on their out-of-plane seismic behavior under varying roof flexibility conditions. Conducted at the EUCENTRE 9D LAB facility in Pavia, Italy, the experimental campaign utilized a dual shake-table testing methodology. This approach allowed for a comprehensive evaluation of the influence of roof stiffness on the seismic response of masonry gables while ensuring boundary conditions that can be replicated in numerical models.

The tests, performed on full-scale masonry gables with three different roof stiffness configurations (Gable 1-STIFF, Gable 2-SEMIFLEX, and Gable 3-FLEX), identified key factors

affecting their seismic vulnerability. Increased roof flexibility resulted in lower seismic capacity and amplified seismic forces on the gables, leading to more earlier collapse compared to stiffer roof configurations. The data obtained from this study provide valuable insights for calibrating numerical models and enhancing existing methods for assessing the seismic performance of URM gables. These models will contribute to more accurate seismic risk evaluations in regions susceptible to both natural and induced seismic activity.

Furthermore, the experimental setup and methodologies employed, including the innovative 9D LAB system at EUCENTRE, established a foundation for future research on masonry structures. The knowledge gained from this work supports the development of improved guidelines and simplified models for assessing the out-of-plane seismic response of URM gables, with potential applications for enhancing seismic safety in earthquake-prone areas worldwide.

ACKNOWLEDGEMENTS

The work presented in the present report is part of the transnational access project "ERIES-SUPREME", supported by the Engineering Research Infrastructures for European Synergies (ERIES) project (www.eries.eu), which has received funding from the European Union's Horizon Europe Framework Programme under Grant Agreement No. 101058684. This is ERIES publication number C78. Additional funding beyond the scope of ERIES was provided by the Ministry of Economic Affairs and Climate (Ministerie van Economische Zaken, EZK) through the Netherlands Organisation for Applied Scientific Research (TNO), under contract number 3100404105 "Wandenaanpak/TU Delft.

REFERENCES

[1] J. Ingham, M. Griffith, Performance of unreinforced masonry buildings during the 2010 Darfield (Christchurch, NZ) earthquake. *Australian Journal of Structural Engineering, 11*(3), 207-224, 2010.

[2] D. Dizhur, J. Ingham, L. Moon, M. Griffith, A. Schultz, I. Senaldi, ..., P. Lourenco, Performance of masonry buildings and churches in the 22 February 2011 Christchurch earthquake. *Bulletin of the New Zealand Society for Earthquake Engineering*, *44*(4), 279-296, 2011.

[3] A. Penna, P. Morandi, M. Rota, C. F. Manzini, F. Da Porto, G. Magenes, Performance of masonry buildings during the Emilia 2012 earthquake. *Bulletin of Earthquake Engineering, 12*, 2255-2273, 2014.

[4] L. Sorrentino, L. Liberatore, D. Liberatore, R. Masiani, The behaviour of vernacular buildings in the 2012 Emilia earthquakes. *Bulletin of Earthquake Engineering*, *12*, 2367-2382, 2014.

[5] P. X. Candeias, A. C. Costa, N. Mendes, A. A. Costa, P. B. Lourenço, Experimental assessment of the out-of-plane performance of masonry buildings through shaking table tests. *Int. J. Archit. Herit.*, 1–28, 2016.

[6] U. Tomassetti, A. A. Correia, F. Graziotti, A. Penna, Seismic vulnerability of roof systems combining URM gable walls and timber diaphragms. *Earthq. Eng. Struct. Dyn.*, 48, 1297–1318, 2019.

[7] M. C. Griffith, N. T. K. Lam, J. L. Wilson, K. Doherty, Experimental investigation of unreinforced brick masonry walls in flexure. *J. Struct. Eng.*, 130(3), 423–432, 2004.

[8] O. Penner, K. J. Elwood, Out-of-plane dynamic stability of unreinforced masonry walls in one-way bending: Parametric study and assessment guidelines. *Earthq. Spectra*, 32, 1699–1723, 2016.

[9] M. Giaretton, D. Dizhur, J. M. Ingham, Dynamic testing of as-built clay brick unreinforced masonry parapets. *Eng. Struct.*, 127, 676–685, 2016.

[10] F. Graziotti, U. Tomassetti, A. Penna, G. Magenes, Out-of-plane shaking table tests on URM single leaf and cavity walls. *Eng. Struct.*, 125, 455–470, 2016.

[11] S. Sharma, U. Tomassetti, L. Grottoli, F. Graziotti, Two-way bending experimental response of URM walls subjected to combined horizontal and vertical seismic excitation." *Eng. Struct.*, 219, 110537, 2020.

[12] U. Tomassetti, L. Grottoli, S. Sharma, F. Graziotti, Dataset from dynamic shake-table testing of five full-scale single leaf and cavity URM walls subjected to out-of-plane two-way bending. *Data Brief*, 24, 103854, 2019.

[13] S. Sharma, L. Grottoli, U. Tomassetti, F. Graziotti, Dataset from shake-table testing of four full-scale URM walls in a two-way bending configuration subjected to combined out-of-plane horizontal and vertical excitation. *Data Brief*, 31, 105851, 2020.

[14] N. Damiani, F. Graziotti, F. Messali and S. Sharma. Out-of-plane shake-table tests on full-scale URM gables considering different roof configurations (ERIES-SUPREME). *Built Environment Data*, 2024. DOI: 10.60756/euc-1avy7q49

[15] European Committee for Standardization (CEN). Methods of test for mortar for masonry. Part 11: Determination of flexural and compressive strength of hardened mortar. European Standard EN 1015-11, Brussels, Belgium, 2006.

[16] European Committee for Standardization (CEN). Methods of test for masonry units. Part 1: Determination of compressive strength. European Standard EN 772-1, Brussels, Belgium, 2011.

[17] European Committee for Standardization (CEN). Methods of test for masonry. Part 1: Determination of compressive strength. European Standard EN 1052-1, Brussels, Belgium, 1998.

[18] European Committee for Standardization (CEN). Methods of test for masonry. Part 5: Determination of bond strength by the Bond Wrench method. European Standard EN 1052-5, Brussels, Belgium, 2005.

[19] European Committee for Standardization (CEN). Methods of test for masonry units. Part 3: Determination of initial shear strength. European Standard EN 1052-3, Brussels, Belgium, 2007.

[20] S. Sharma, F. Graziotti, G. Magenes. Torsional shear strength of unreinforced brick masonry bed joints. *Constr. Build. Mater*., 275, 122053, 2021.

[21] M. Mirra, N. Damiani, S. Sharma, F. Graziotti, F. Messali. Definition of differential seismic input motions for out-of-plane dynamic testing of unreinforced masonry gable walls considering different roof configurations. *Structures*, 2025.

[22] M. Kohrangi, P. Bazzurro, D. Vamvatsikos and A. Spillatura, Conditional spectrum-based ground motion record selection using average spectral acceleration. *Earthq. Eng. Struct. Dyn.*, 46: 1667–1685, 2017.